



Nature-based solutions enhanced by reactive materials for the protection of urban water bodies

Agnieszka Bus*, Agnieszka Karczmarczyk, Anna Baryła

Institute of Environmental Engineering, Warsaw University of Life Sciences – SGGW, Nowoursynowska 159, 02-776 Warszawa, Poland, emails: agnieszka_bus@sggw.edu.pl (A. Bus), agnieszka_karczmarczyk@sggw.edu.pl (A. Karczmarczyk), anna_baryla@sggw.edu.pl (A. Baryła)

Received 14 March 2022; Accepted 6 August 2022

ABSTRACT

Nature-based solutions (NBS) are defined as supported and inspired by nature solutions that are cost-effective and simultaneously provide environmental, social and, economic benefits that help build resilience. In the case of water resources, NBS increases the quantity of water resources but also, on the other hand, contributes to water quality improvement by limiting and inhibiting of eutrophication process. The study aimed to assess the efficiency of opoka rock (carbonate-siliceous rock) for phosphorus (P) removal and pointed out its potential application in NBS for urban water bodies protection. The batch reactor studies were taken for three different initial P-PO₄ concentrations: 0.996, 5.113 and 10.815 mg/L, corresponding to removal after 91 h of 82%, 90%, and 93%. The research investigated also sorption mechanisms by different kinetic models: pseudo-first-order and pseudo-second kinetic order models, Elovich and intraparticle diffusion model. Obtained results were characterized by the highest fit to the pseudo-second kinetic and Elovich models. The implementation aspect of the presented studies is the nomogram for estimating reactive material mass vs. initial P-PO₄ concentration.

Keywords: Kinetic models; Nature-based solutions; Phosphorus; Reactive materials; Water treatment

1. Introduction

Numerous anthropogenic activities in urbanized areas have impacted on aquatic ecosystems and led to the deterioration of water quality. The impact of urban pollution on water bodies has been well described in the literature [1–8]. Different kinds of pollutants constantly supply urban surface waters. Among the vast array of contaminations occurring in urbanized areas, such as heavy metals, polycyclic aromatic hydrocarbons, herbicides, organic compounds, and bacterial indicators [9], there are also nutrients such as nitrogen (N) and phosphorus (P) species causing a harmful effect to aquatic ecosystems. Excessive

nutrient loads, especially P, consequently lead to eutrophication of water bodies. There is no exact value above which waters are exposed to eutrophication. However, European Council Directive 91/271/EEC [10] states that if a P-PO₄ concentration in river water exceeds 0.1 mg/L, it is excessively enriched with P. The relationship between P export and urbanization has been previously examined [2,3]. The primary sources of P in urban areas are natural (i.e., atmospheric deposition), anthropogenic (i.e., fertilization, animal wastes), or biogenic materials (i.e., lawn clippings and leaves) [3,6,8]. The P concentration in urban areas may range from 0.43 mg/L from medium and high-density single family residential [7] to even 1.27 mg/L

* Corresponding author.

from single family residential neighborhoods [6]. Also, the P load exported to urban water bodies may differ significantly. Yang and Toor [8] noted that P export from a small urban watershed in Maryland ranged from 24.5 to 83.7 kg/km²/y. Toor et al. [6] observed an average P load of 0.44 kg/d from urban runoff in a residential neighborhood.

One of the ways to improve water quality in urban areas is to implement nature-based solutions (NBS). Generally, such solutions are defined as supported and inspired by nature, cost-effective, and simultaneously provide environmental, social and economic benefits that help build resilience [11]. NBS enhances natural features and processes occurring to combat among others climate change, reduce flood risk, improve water quality, protect and stabilize coastal areas, restore and protect wetlands or provide recreation areas [12]. Generally, NBS reduces the levels of such primary pollutants as suspended soils, organic matter, heavy metals and nutrients. Due to the presence of aquatic plants, the most preferred nutrient to reduce is N [13]. P accumulation by plants is relatively low, but it should be remembered that removing such nutrients is not the primary treatment target of NBS [14,15]. For this reason, to remove P simultaneously by different kinds of NBS, such solutions should be enhanced by appropriate reactive material (RM). RMs dedicated to P removal should contain Al, Ca, Ce, Fe, La, Mg, Zn, and Zr in their composition [16]. P harvesting occurs during treatment process such as physiochemical methods, biological treatment processes, ion exchange, electro-coagulation, and sorption, among which P can be removed. However, the most popular approach is sorption because of optimal cost and easy maintenance [17].

The study aimed to (1) assess the efficiency of opoka rock (carbonate–siliceous rock) for phosphorus (P) removal, (2) create the nomogram connecting the mass of reactive material with initial P concentration, and (3) point out potential RM application in NBS for protection of urban water bodies.

Kinetic studies are a popular way of testing the sorption properties of RMs with the function of increasing time. This research introduces a novel method for linking the results obtained from kinetic studies with practical implementation by a nomogram using to define the mass of RM in the case of initial P concentration. Such a solution is proper, especially from a practical point of view, and provides information about the sorption properties of materials. Using nomograms is helpful to support NBS in P removal as a best available practice for preventing P excess in urban water bodies and eutrophication.

2. Materials and methods

2.1. Reactive material

Reactive material (RM) used in studies is thermal treated at 900°C carbonate–siliceous rock called opoka. Because of respectively high contamination of Ca (Table 1) this material is potentially phosphorus-reactive. The following standards were used to determine the physical properties of RM: particle size distribution PN EN 933-1:2012 and PN-ISO 11277:2005, bulk density PN EN 1097-3:2000, porosity PN-EN 1936:2010. pH was determined by

VOLCRAFT PH-212 meter. The composition of the materials was analyzed on a Philips X'Pert PW 3020 X-ray diffractometer. The main parameters characterizing the RM are set in Table 1.

2.2. Batch reactor tests

Three different P–PO₄ concentrations (0.996, 5.113, and 10.815 mgP–PO₄/L) made of KH₂PO₄ were used for kinetic studies with varying contact times ranged from 5 min to 5,460 min (91 h). The 0.5 g of RM was mixed with 50 mL of artificial P–PO₄ solution at a speed of 96 rpm at a stable temperature of 20°C. The experiment was performed in four replications.

The removal ratio R (%) was calculated based on the formula:

$$R = \frac{C_0 - C_e}{C_0} \times 100 \quad (1)$$

where C_0 and C_e are the initial and equilibrium P–PO₄ concentrations (mg/L).

The sorption capacity (mg/g) was calculated from the formula:

$$S = \frac{(C_0 - C_e) \cdot V}{m} \quad (2)$$

where S is the sorption capacity (mg/g); V is the volume of solution (L); m is the mass of RM (g), and C_0 and C_e are the initial and equilibrium P–PO₄ concentrations (mg/L).

The P–PO₄ concentration was analyzed with the ammonium molybdate method in a FIAstar 5000 Analyzer in two ranges of 0.005 to 1 mgP–PO₄/L and 0.1 to 5 mgP–PO₄/L depending on the phosphate concentration. Before determination, the samples were filtered by a syringe filter of 0.45 μm pore size.

2.3. Kinetic models

To better understand the mechanism of adsorption kinetic, four different kinetic models were used: pseudo-first-order and, pseudo-second-order kinetic models, Elovich and intraparticle diffusion model.

The equalizations of the following models are presented below:

Pseudo-first-order kinetic model proposed by Lagergren [19]:


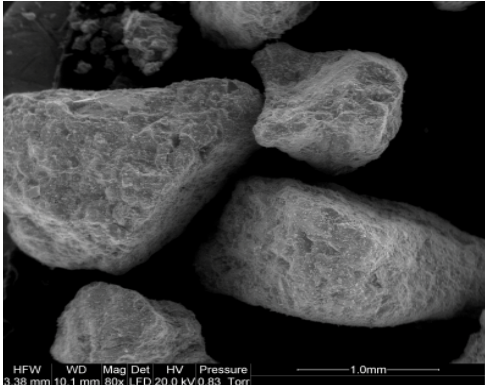
$$\log(q_e - q_t) = \log(q_e) - \frac{k_1}{2.303} t \quad (3)$$

where q_t (mg/g) represents the amount of P adsorbed at any time t (min), k_1 (min⁻¹) is a constant rate of sorption of the pseudo-first kinetic model and q_e is the amount adsorbed at equilibrium (mg/g).

Pseudo-second-order kinetic model, also called the Ho model [20]:

$$\frac{t}{q_t} = \frac{1}{(k_2 q_e^2)} + \frac{1}{q_e} t \quad (4)$$

Table 1
Characteristics of tested RM

Thermal treated opoka	SEM photography
	
Main chemical components (%): SiO ₂ – 55; CaO – 24; Al ₂ O ₃ – 6; Fe ₂ O ₃ – 3	
Grain size (mm)	2.0–5.0
pH (–)	10.8
Bulk density (g/cm ³)	0.75
Porosity (%)	38.0
S _{max} (mgP-PO ₄ /g)	95.70 [18]

where q_t (mg/g) represents the amount adsorbed at any time t (min), k_2 (g/mg·min) is a constant rate of sorption of the pseudo-second kinetic model and q_e is the amount adsorbed at equilibrium (mg/g).

Elovich model [21]:

$$q_t = \frac{1}{\beta} \ln(\alpha\beta) + \frac{1}{\beta} \ln(t) \quad (5)$$

where q_t (mg/g) represents the amount adsorbed at any time t (min). α (mg/g·min) is the initial sorption rate and parameter β (g/mg) is related to the extent of surface coverage and activation energy for chemisorption.

Intraparticle diffusion model [22]:

$$q_t = k_d t^{0.5} + C \quad (6)$$

where q_t (mg/g) represents the amount adsorbed at any time t (min), k_d (mg/g·min^{0.5}) is a constant rate of sorption of the intraparticle diffusion model. C is a boundary layer thickness. The higher the value, the greater the effect.

All constants were calculated based on slopes and intercepts of the linear formula of each tested kinetic model. The linearized form of equations with plots and formulas to calculate the constants are set in Table 2.

2.4. Practical applications

The practical implementation of tested material to support and enhanced NBS is presented in Fig. 1.

The first step of the methodology includes the batch reactor kinetic studies with an evaluation of specific kinetic model parameters.

In the second step, the nomogram of RM mass vs. initial P concentrations is created based on the average slope of the straight lines for tested concentrations (~1, 5, and 10 mg/L) in the time necessary to achieve equilibrium (till 900 min).

Finally, the third step presents the potential application of RM focused on the protection and improvement of water bodies conditions in urban areas by enhancing NBS.

3. Results and discussion

3.1. Sorption capacity

Adsorption kinetic studies have to be conducted before the practical implementation of RM and thanks to this the behavior and potential sorption capacity can be defined.

The contact time of the material with the solution strongly affected the P-PO₄ concentrations and decreased with prolonged reaction time (Fig. 2a). After the retention time of 91 h, the final P-PO₄ concentration equalled 0.176 mg/L (SD 0.000), 0.493 mg/L (SD 0.047) and 0.698 mg/L (SD 0.002) for 1, 5 and 10 mg/L, respectively. The final concentrations of P-PO₄ obtained after 91 h of contact time have a good correlation ($R^2 = 0.974$) with initial concentrations. Such observation was also noted in previous papers [18,23]. Next, the obtained concentrations were recalculated according to the Eq. (2) into removal ratio (R) and presented in Fig. 2b. At the end of the experiment, the removal ratio was 82% (SD 0.000), 90% (SD 0.266), and 93% (SD 0.016) for 1, 5, and 10 mg/L, respectively. A faster R value was observed in the case of higher initial concentrations. This phenomenon is explained as in lower concentrations, only adsorption occurs. In higher,

Table 2
Parameters of tested kinetic models

Kinetic model	Plots	Slopes	Intercepts
Pseudo-first-order	$\log(q_e - q_t)$ vs t	$-\frac{k_t}{2.303}$	$\log(q_e)$
Pseudo-second-order	$\frac{t}{q_t}$ vs t	$\frac{1}{q_e}$	$\frac{1}{kq_e^2}$
Elovich	q_t vs $\ln(t)$	$\frac{1}{\beta}$	$\frac{1}{\beta} \ln(\pm\beta)$
Intraparticle diffusion	q_t vs $t^{\frac{1}{2}}$	k_d	C

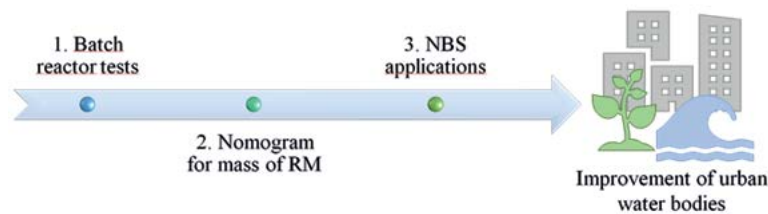


Fig. 1. Stepwise procedure for practical application of obtained results.

apart from adsorption, also complexation and precipitation take place [23,24]. Opoka obtained the equilibrium stage faster for higher concentrations (5 and 10 mg/L) than lower (1 mg/L). It is well seen in the case of Fig. 2b with the P-PO₄ removal ratio. For 5 and 10 mg/L, the removal started to slow down and stabilized after 900 min of contact time. In the case of 1 mg/L concentration, the reduction stabilized after 4,260 min of contact time, so it is more than four times longer than for 5 and 10 mg/L. The correlation R^2 between initial P-PO₄ concentrations and obtained removal ratio after 91 h is 0.943.

The obtained concentrations were also recalculated into sorption (S) by Eq. (3) and presented in Fig. 3. The course of the process of P sorption from the solution at a variable time is shown in Fig. 2. The final P-PO₄ sorption obtained in this study equaled 0.084 mg/g (SD 0.000), 0.464 mg/g (SD 0.005), and 1.018 mg/g (SD 0.000), for 1, 5, and 10 mg/L, respectively.

Considering Figs. 2 and 3, there are well seen three stages of the removal process. The first stage showed a sharp and rapid reaction that lasted the first 60 min of contact time with RM. During this stage 36%, 36%, and 30% of P were removed from the solution by 1, 5, and 10 mg/L concentration, respectively (Fig. 2), corresponding to sorption equaled 0.037, 0.192 and 0.334 mgP-PO₄/g, respectively. The high removal rate at the first stage may result from of an increasing number of vacant sites available at the initial adsorption phase. Consequently, increased concentrations of gradients between adsorbate in solution and adsorbate in RM surface [22]. The second stage lasts 900 min and shows gradual adsorption completed with the removal of 94%,

91%, and 91% of P from the solution by 1, 5, and 10 mg/L concentration, respectively (Fig. 2b). The observed sorption equaled 0.056 0.418 and 0.980 mgP-PO₄/g. In the third, final equilibrium stage, where due to extremely low adsorbate concentrations in the solution, the removal rate slows down and remains constant (Fig. 2b). Up to 91%–94% of the initial concentration of P uptake was found to occur in this stage. During this time, the sorption rate started to slow down and stabilized. The sorption equaled 0.082 (SD 0.000), 0.462 (SD 0.005) and 1.011 (SD 0.000) mgP-PO₄/g for 1, 5 and 10 mg/L, respectively. Also, the obtained final sorption results are in good agreement (R^2) with initial P-PO₄ concentrations equaled 0.999.

In a previous study [18], the sorption properties of opoka were tested in an isotherm test. Two different isotherm models, Langmuir and Freundlich, were developed to obtain sorption properties with increasing P-PO₄ concentrations ranging from 1 to 1,000 mg/L and a constant contact time of 24 h. The data were characterized by better fitting to the Langmuir model and maximum adsorption capacity (S_{max}) equaled 95 mgP-PO₄/g.

The results of constant parameters with coefficients of determination are set in Table 3. Considering the obtained results, the highest fitting (0.9894–0.9997) was obtained in the case of the pseudo-second-order model for all tested concentrations. A slightly lower fit is seen in the case of the Elovich model (0.9894–0.9997). The degree of fitting in the case of both models increases with the initial P concentration. For others tested kinetic models, the R^2 ranged from 0.7247 to 0.9410 and from 0.7627 to 0.9496 for pseudo-first-order and intraparticle diffusion models, respectively.

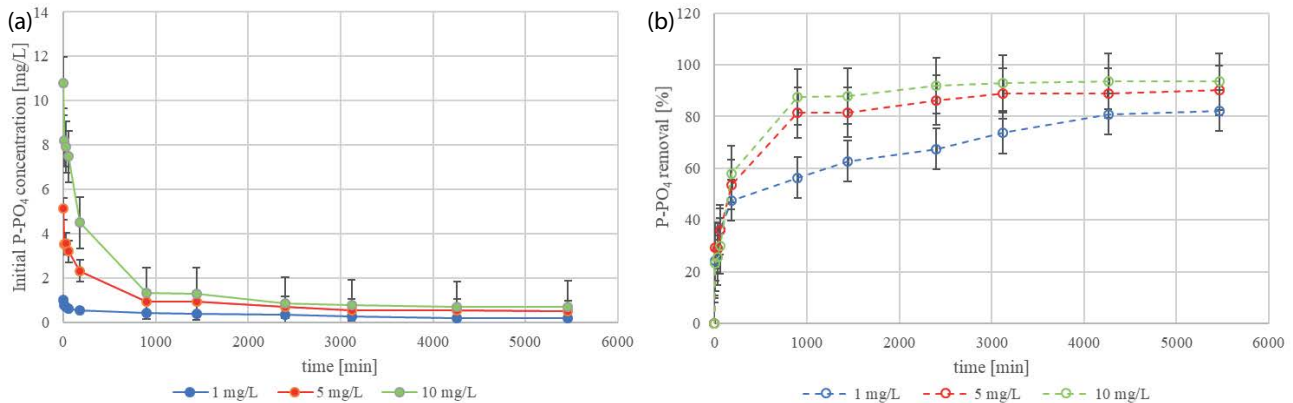


Fig. 2. Decreasing of the average phosphate concentration (a) and the average removal ratio (b) in time. Whispers indicate standard deviation (SD).

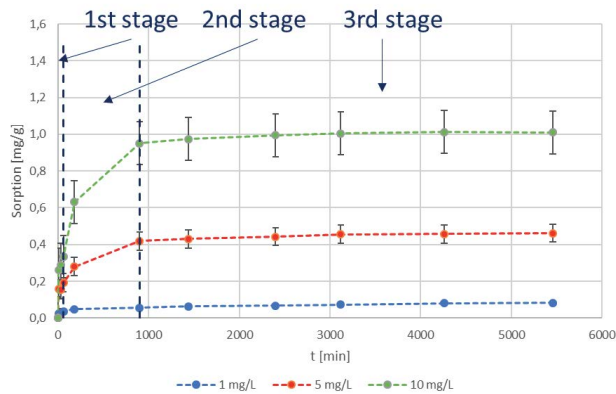


Fig. 3. Average P-PO₄ sorption for opoka. The vertical line indicates the stages (1st, 2nd and 3rd stage). Whispers indicate standard deviation.

The high level of fitting of the obtained data to the pseudo-second-order model agrees with chemisorption. Moreover, the good agreement with the Langmuir isotherm model obtained in the previous study [18] also proclaims this statement [25,26]. Chemisorption occurs when a chemical's functional group interacts with a reactive surface on the RMs through the formation of strong chemical bonds [17]. The pseudo-second-order model is based on the sorption capacity of the solid phase of RM. The rate-limiting step is the surface adsorption that involves chemisorption, where the removal from a solution is due to physicochemical interactions between the two phases [17]. In addition, the examined data is also characterized by good fitting to the Elovich model (Table 3), suggesting that chemisorption also controls the adsorption [25]. Chemisorption is a process that involves the transfer of electrons between the adsorbate and adsorbent [26]. However, recognizing the sorption process cannot only be defined by fitting to the pseudo-second-order model [27,28]. The pseudo-second-order process depends on dose amount, pH, temperature, and particle size [29,30]. Moreover, Kajjumba et al. [25] claim that the pseudo-second-order adsorption

Table 3
Results of examined kinetic models

Specification	Initial P-PO ₄ concentration (mg/L)		
	0.996	5.113	10.815
Experimental q_e (mg/g)	0.084	0.464	1.018
Pseudo-first-order model			
k_1 (min ⁻¹)	0.000013	0.000017	0.000022
q_e (mg/g)	0.062	0.240	0.469
R^2 (-)	0.9410	0.7730	0.7247
Pseudo-second-order model			
k_2 (g/mg·min)	0.0588	0.0239	0.0117
q_e (mg/g)	0.0819	0.4667	1.0283
R^2 (-)	0.9894	0.9995	0.9997
Elovich model			
α	0.0078	0.0388	0.0830
β	117.65	18.73	7.55
R^2	0.9563	0.9421	0.9337
Intraparticle diffusion model			
k_d (mg/g·min ^{0.5})	0.0007	0.0041	0.0097
C (mg/g)	0.0308	0.1985	0.3942
R^2 (-)	0.9469	0.8101	0.7627

mechanism is favored at low initial concentrations. On the contrary, at high initial concentration, the pseudo-first-order model seems to be dominant because at low C_0 the value of $\log(q_e - q_t)$ increases exponentially, increasing the error function that is the reverse for high C_0 .

3.2. Implementations guidelines

The average slopes of the lines leveling the concentrations in the time needed to achieve equilibrium (Fig. 4 left) were used to create a nomogram (Fig. 4 right). A nomogram is a graph of dependencies between variables presented on

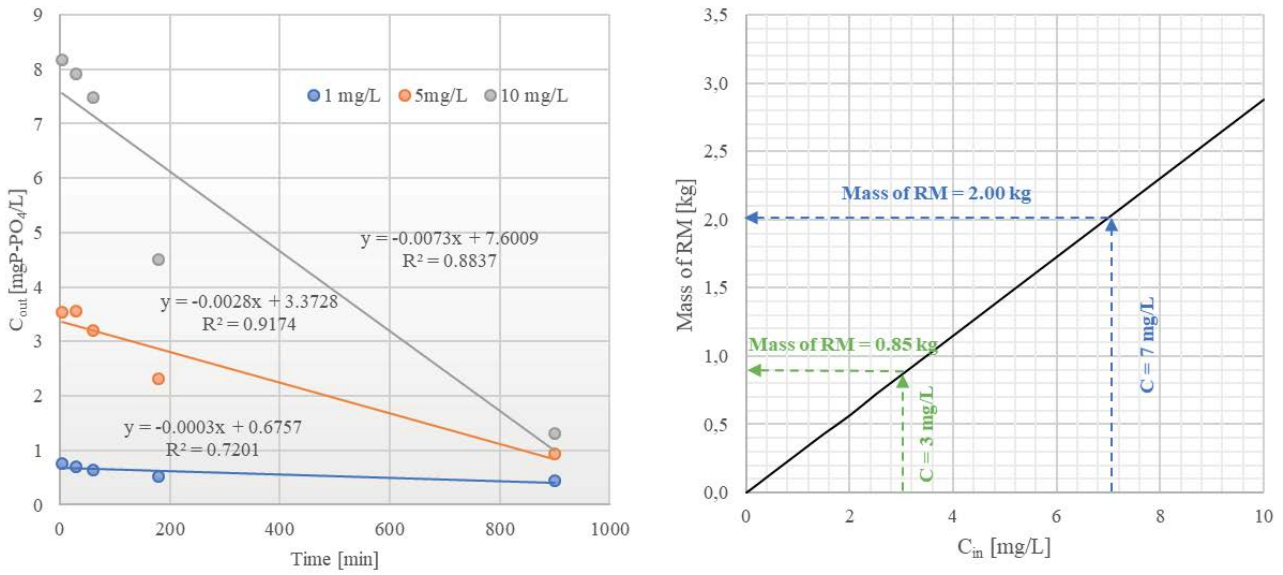


Fig. 4. Changing the final phosphate concentrations in equilibrium time (left) and predictive nomogram for the mass of reactive material needed to reduce the initial concentration of 92% for mass to volume ratio of 10 g:1 L.

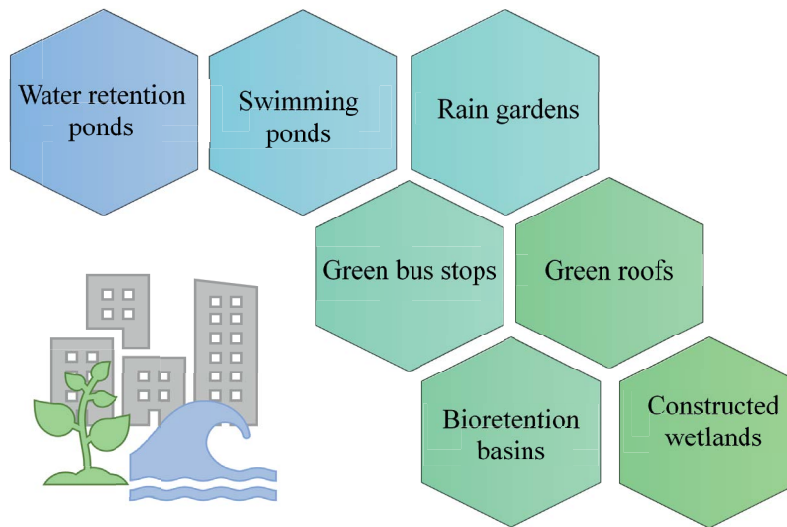


Fig. 5. Potential applications of RMs reducing P and enhancing NBS for urban water bodies protection.

separate scales (x -axis), enabling the search variable's readout using the graphic method (y -axis). According to the nomogram, we can predict the mass of RM needed to remove 92% of P concentration ranged from 1 to 10 mg/L with a mass to volume ratio of 10 g:1 L. For example, for an initial concentration of 3 mg/L, 0.85 kg of material is needed to remove the concentration to the final level of 0.24 mg/L. In the case of P removal from the initial level of 7 mg/L, 2.0 kg of RM is needed to reduce the concentration to 0.23 mg/L, etc. Such solution was previously used to estimate the permeable reactive barrier [18], the relationship between constructed wetland area and mass of RM required to achieve outlet concentration of 0.01 mgP/L [31], predicting slag mass in dependence of retention time [32] or predicting oxygen uptake

rate in dependence of BOD_5/TP and sludge concentration in a biological reactor [33].

This study discussed using of RMs to control P concentration in bodies of water receiving urban runoff. RM present a wide array of potential applications shown in Fig. 5. It can be applied in swimming ponds or water retention ponds to keep the P concentration at levels that limit algae growth and ensure safe use [34,35]. Green roofs and bus stops have been starting a popular solution to increase the amount of green in the cities, reduce surface runoff and increase the retention of rainfall in urban areas. In this case, RMs can be used as an underlined substrate drainage layer to reduce the P load from substrate and fertilizers used to ensure the growth of plants [36]. Another option

is to enhance rain gardens with RMs to limit P concentrations discharged into the environment [37]. A bio-retention basin is an area densely covered with vegetation where rainwater is collected, which cleans by seeping through subsequent substrate layers [38] that may also be supported by RMs [39]. Using them enhances the natural treatment process and makes it much more effective because temporarily water drying may support the P regeneration of RM, especially based on Ca [34]. RMs may also enhance free water surface constructed wetlands treating river water or stormwater in urbanized areas. Using RMs can minimize the wetland area necessary to remove an excess of P [31].

4. Conclusion

Based on the conducted research, there is well seen an influence of initial P-PO₄ concentration on obtained final concentration, removal ratio, and sorption after 91 h of contact time. At the end of the experiment, the removal ratio equalled 82%, 90%, and 93% for 1, 5, and 10 mg/L, respectively. These correspond to the unit sorption of 0.082, 0.462 and 1.011 mgP-PO₄/g for 1, 5 and 10 mg/L, respectively.

The obtained data are characterized by the best fitting to the pseudo-second kinetic order (R^2 ranged from 0.9894 to 0.9997) and the Elovich model (R^2 ranged from 0.9337 to 0.9653), which suggest that chemisorption may be a dominant P-PO₄ removal process.

The practical implementation of obtained data was the nomogram created to predict the final mass of RM depending on the initial P-PO₄ concentration. Such a solution can increase NBS effectiveness in P harvesting from urban water bodies, which are highly endangered by the eutrophication process.

References

- [1] K. Glińska-Lewczuk, I. Gołaś, J. Koc, A. Gotkowska-Płachta, M. Harnisz, A. Rochwerger, The impact of urban areas on the water quality gradient along a lowland river, *Environ. Monit. Assess.*, 188 (2016) 624, doi: 10.1007/s10661-016-5638-z.
- [2] M.A. Mallin, V.L. Johnson, S.H. Ensign, Comparative impacts of stormwater runoff on water quality of an urban, a suburban, and a rural stream, *Environ. Monit. Assess.*, 159 (2009) 475–491.
- [3] S.E. Hobbie, J.C. Finlay, B.D. Janke, D.A. Nidzgorski, D.B. Millet, L.A. Baker, Contrasting nitrogen and phosphorus budgets in urban watersheds and implications for managing urban water pollution, *Proc. Natl. Acad. Sci.*, 114 (2017) 4177–4182.
- [4] J. Pokryvková, L. Jurík, L. Lackóová, K. Halászová, R. Hanzlík, M.E. Banihabib, The urban environment impact of climate change study and proposal of the city micro-environment improvement, *Sustainability*, 13 (2021) 4096, doi: 10.3390/su13084096.
- [5] T. Correia, M. Regato, A. Almeida, T. Santos, L. Amaral, M. de Fátima Nunes Carvalho, Manual treatment of urban wastewater by chemical precipitation for production of hydroponic nutrient solutions, *J. Ecol. Eng.*, 21 (2020) 143–152.
- [6] G.S. Toor, M.L. Occhipinti, Y.-Y. Yang, T. Majcherek, D. Haver, L. Oki, Managing urban runoff in residential neighborhoods: nitrogen and phosphorus in lawn irrigation driven runoff, *PLoS One*, 12 (2017) e0179151, doi: 10.1371/journal.pone.0179151.
- [7] Y.-Y. Yang, G.S. Toor, Sources and mechanisms of nitrate and orthophosphate transport in urban stormwater runoff from residential catchments, *Water Res.*, 112 (2017) 176–184.
- [8] Y.-Y. Yang, G.S. Toor, Stormwater runoff driven phosphorus transport in an urban residential catchment: implications for protecting water quality in urban watersheds, *Sci. Rep.*, 8 (2018) 11681, doi: 10.1038/s41598-018-29857-x.
- [9] E. Eriksson, A. Baun, L. Scholes, A. Ledin, S. Ahlman, M. Revitt, C. Noutsopoulos, P.S. Mikkelsen, Selected stormwater priority pollutants – a European perspective, *Sci. Total Environ.*, 383 (2007) 41–51.
- [10] Council Directive of 21 May 1991 Concerning Urban Wastewater Treatment (91/271/EEC). Available at: <https://eur-lex.europa.eu/legal-content/EN/TXT/PDF/?uri=CELEX:31991L0271&from=EN> (31.05.2022).
- [11] EU, Towards an EU Research and Innovation Policy Agenda for Nature-Based Solutions and Re-Naturing Cities, European Commission. Available at: <https://op.europa.eu/en/publication-detail/-/publication/fb117980-d5aa-46df-8edc-af367cddc202> (15.02.2022).
- [12] Building Community Resilience With Nature-Based Solutions, A Guide for Local Communities, FEMA June 2021. Available at: https://www.fema.gov/sites/default/files/documents/fema_riskmap-nature-based-solutions-guide_2021.pdf (18.02.2022).
- [13] J. Vymazal, Constructed wetlands for wastewater treatment, *Water*, 2 (2010) 530–549.
- [14] N. Atanasova, J.A.C. Castellar, R. Pineda-Martos, C.E. Nika, E. Katsou, D. Istenič, B. Pucher, M.B. Andreucci, G. Langergraber, Nature-based solutions and circularity in cities, *Circ. Econ. Sustainability*, 1 (2021) 319–332.
- [15] N. Frantzeskaki, Seven lessons for planning nature-based solutions in cities, *Environ. Sci. Policy*, 93 (2019) 101–111.
- [16] H. Bacelo, A.M.A. Pintor, S.C.R. Santos, R.A.R. Boaventura, C.M.S. Botelho, Performance and prospects of different adsorbents for phosphorus uptake and recovery from water, *Chem. Eng. J.*, 381 (2020) 122566, doi: 10.1016/j.cej.2019.122566.
- [17] A. Gizaw, F. Zewge, A. Kumar, A. Mekonnen, M. Tesfaye, A comprehensive review on nitrate and phosphate removal and recovery from aqueous solutions by adsorption, *J. Water Supply Res. Technol. AQUA*, 70 (2021) 921–947.
- [18] A. Bus, A. Karczmarczyka, A. Baryła, Phosphorus reactive materials for permeable reactive barrier filling – lifespan estimations, *Desal. Water Treat.*, 245 (2022) 9–15.
- [19] J.X. Lin, L. Wang, Comparison between linear and non-linear forms of pseudo-first-order and pseudo-second-order adsorption kinetic models for the removal of methylene blue by activated carbon, *Front. Environ. Sci. Eng.*, 3 (2009) 320–324.
- [20] Y.S. Ho, D. McKay, Pseudo-second-order model for sorption processes, *Process Biochem.*, 34 (1999) 451–465.
- [21] A.M. Peers, Elovich adsorption kinetics and the heterogeneous surface, *J. Catal.*, 4 (1965) 499–503.
- [22] V. Vadivelan, K. Vasanth Kumar, Equilibrium, kinetics, mechanism, and process design for the sorption of methylene blue onto rice husk, *J. Colloid Interface Sci.*, 286 (2005) 90–100.
- [23] L. Zhang, J.Y. Liu, L.H. Wan, Q. Zhou, X.Z. Wang, Batch and fixed-bed column performance of phosphate adsorption by lanthanum-doped activated carbon fiber, *Water Air Soil Pollut.*, 223 (2012) 5893–5902.
- [24] Y. Xu, T.J. Liu, Y.K. Huang, J.Y. Zhu, R.L. Zhu, Role of phosphate concentration in control for phosphate removal and recovery by layered double hydroxides, *Environ. Sci. Pollut. Res.*, 27 (2020) 16612–16623.
- [25] G.W. Kajjumba, S. Emik, A. Öngen, H. Kurtulus Özcan, S. Aydın, Modelling of Adsorption Kinetic Processes—Errors, Theory and Application, S. Edebali, Ed., *Advanced Sorption Process Applications*, InTechOpen, 2018, doi: 10.5772/intechopen.80495.
- [26] Y.S. Ho, G. McKay, A comparison of chemisorption kinetic models applied to pollutant removal on various sorbents, *Process Saf. Environ. Prot.*, 76 (1998) 332–340.
- [27] H.J. Wang, A.L. Zhou, F. Peng, H. Yu, J. Yang, Mechanism study on adsorption of acidified multi-walled carbon nanotubes to Pb(II), *J. Colloid Interface Sci.*, 316 (2007) 277–283.
- [28] H.N. Tran, S.-J. You, A. Hosseini-Bandegharai, H.-P. Chao, Mistakes and inconsistencies regarding adsorption of contaminants from aqueous solutions: a critical review, *Water Res.*, 120 (2017) 88–116.

- [29] J.-P. Simonin, On the comparison of pseudo-first-order and pseudo-second-order rate laws in the modeling of adsorption kinetics, *Chem. Eng. J.*, 300 (2016) 254–263.
- [30] E.D. Revellame, D.L. Fortela, W. Sharp, R. Hernandez, M.E. Zappi, Adsorption kinetic modeling using pseudo-first-order and pseudo-second-order rate laws: a review, *Cleaner Eng. Technol.*, 1 (2020) 100032, doi: 10.1016/j.clet.2020.100032.
- [31] A. Bus, A. Karczmarczyk, Supporting constructed wetlands in P removal efficiency from surface water, *Water Sci. Technol.*, 75 (2017) 2554–2561.
- [32] L.H. Wang, C. Penn, C.-h. Huang, S. Livingston, J.H. Yan, Using steel slag for dissolved phosphorus removal: insights from a designed flow-through laboratory experimental structure, *Water*, 12 (2020) 1236, doi: 10.3390/w12051236.
- [33] E. Nowobilska-Majewska, P. Bugajski, The impact of selected parameters on the condition of activated sludge in a biologic reactor in the treatment plant in Nowy Targ, Poland, *Water*, 12 (2020) 2657, doi: 10.3390/w12102657.
- [34] A. Karczmarczyk, A. Bus, A. Baryła, Influence of operation time, hydraulic load and drying on phosphate retention capacity of mineral filters treating natural swimming pool water, *Ecol. Eng.*, 130 (2019) 176–183.
- [35] A. Bańkowska-Sobczak, Calcite as a candidate for non-invasive phosphorus removal from lakes, *Ecohydrol. Hydrobiol.*, 21 (2021) 683–699.
- [36] A. Baryła, A. Karczmarczyk, A. Brandyk, A. Bus, The influence of a green roof drainage layer on retention capacity and leakage quality, *Water Sci. Technol.*, 77 (2018) 2886–2895.
- [37] M.E. Dietz, J.C. Clausen, Saturation to improve pollutant retention in a rain garden, *Environ. Sci. Technol.*, 40 (2006) 1335–1340.
- [38] M. Eadie, *Water Sensitive Urban Design for the Coastal Dry Tropics (Townsville): Design Objectives for Stormwater Management*, Townsville City Council, 2011. Available at: https://www.townsville.qld.gov.au/__data/assets/pdf_file/0007/12220/Design_Objectives_For_Stormwater_Management.pdf (16.02.2022).
- [39] C. Berretta, A. Aiello, H.S. Jensen, M.R. Tillotson, A. Boxall, V. Stovin, Influence of Design and Media Amendments on the Performance of Stormwater Biofilters, *Proceedings of the Institution of Civil Engineers-Water Management*, Thomas Telford Ltd., 2018, pp. 87–98.